Electronic Supplementary Material (ESI) for Journal of Materials Chemistry A.
This journal is © The Royal Society of Chemistry 2020

Supplementary Information

Superhydrophobic, Multi-Responsive and Flexible Bottlebrush-Network-based Form-Stable Phase Change Materials for Thermal Energy Storage and Sprayable Coating

Supplementary Experiment

Measurements:

Gel permeation chromatography (GPC) were carried out in THF with flow rate of 1.0 ml/min and column temperature at 40°C by Water 1515 liquid chromatograph equipped with Water 2414 refractive index detector to obtain the molecular weight of the polymers. Polystyrene standards were used for calibration.

Abrasion tests were carried out by using a counterweight with a diameter of 2.2 cm and a mass of 100 g under a piece of 1000-grit attached sandpaper (25 mm × 25 mm). The film sample (75 mm × 25 mm) for abrasion was clamped down and abraded at 50 cycles/min under 1.57 kPa pressure. A new sandpaper was replaced every 5 cycles and each moving length is 5 cm.

The crystalline properties of $Si_{Pa\text{-}x}$ were also characterized by POM using Olympus BX51 polarizing microscope.

The thermal mechanical and mechanical properties were measured by dynamic mechanical analyzer (DMA, Q800, TA instrument). The specimen (30 mm × 6 mm × 1 mm) was examined at a constant frequency of 1 Hz, at the temperature ranging from

-140 to 100 °C, with a heating rate of 3 °C /min in air atmosphere.

The leakage tests were carried out as following: each sample along with the white A4 paper was put into an oven at the temperature of 100 °C and kept for 30 min to make sure the melting. After cooling to around 25 °C, all the samples were removed from the white paper. At last, each piece of the white paper was carefully examined to find out whether there were any liquid traces left on it or not. Besides, the masses of samples were compared before and after the leakage test to further find out if the leakage problem existed in this system.

Supplementary Figures

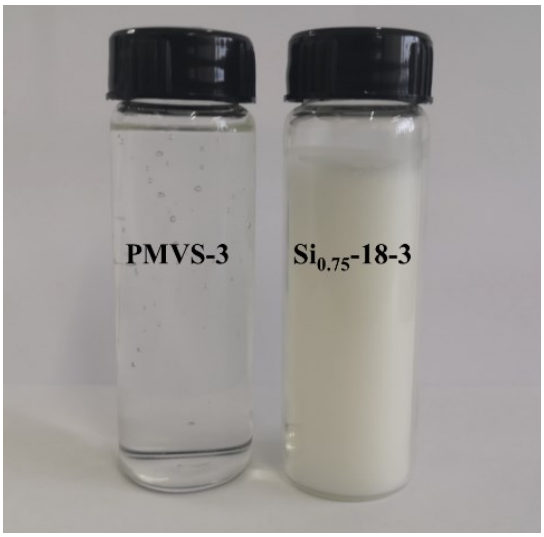

Figure S1 Optical images of PMVS-3 and $Si_{0.75}$-18-3.

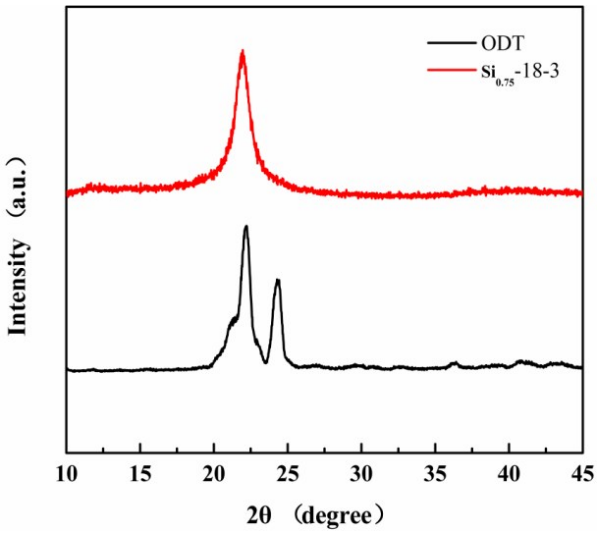

Figure S2 X-ray diffraction diagrams of for $Si_{0.75}$-18-3 and ODT.

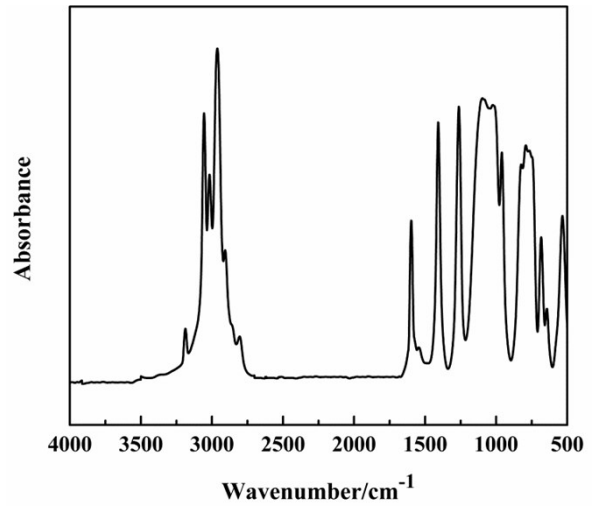

Figure S3 Fourier transform infrared (FT-IR) spectra of PVMS-1.

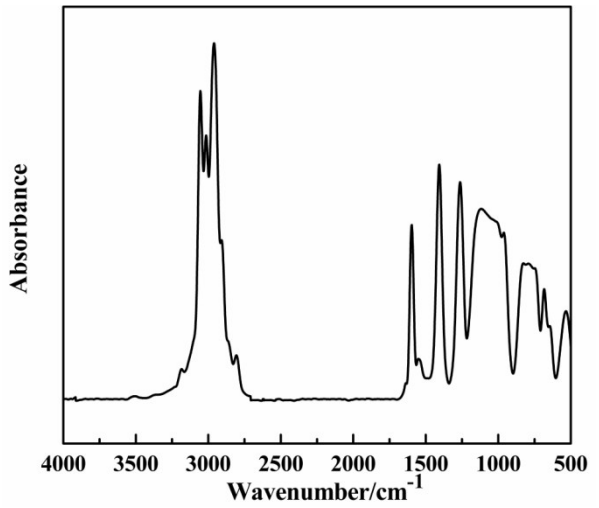

Figure S4 Fourier transform infrared (FT-IR) spectra of PVMS-2.

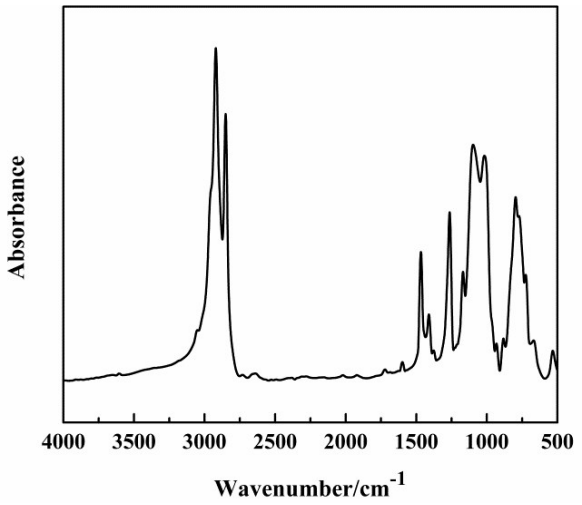

Figure S5 Fourier transform infrared (FT-IR) spectra of $Si_{0.75}$-18-1.

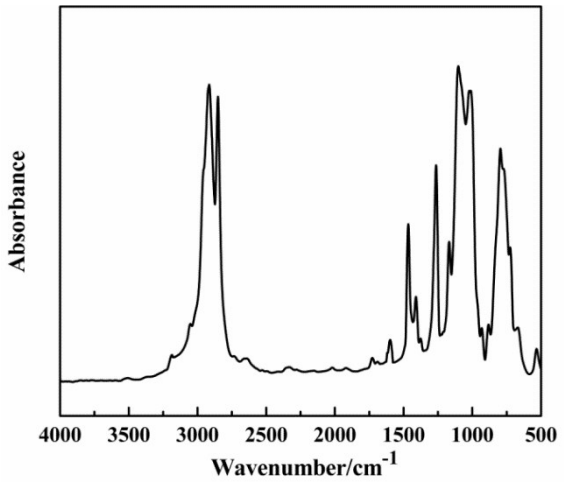

Figure S6 Fourier transform infrared (FT-IR) spectra of $Si_{0.75}$-18-2.

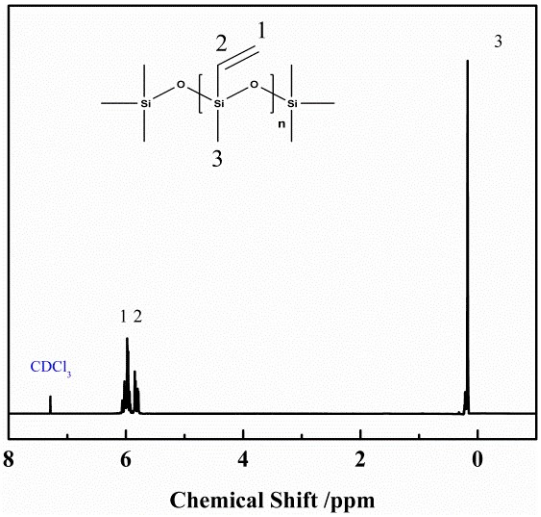

Figure S7 ^{1}H NMR spectrum of PVMS-3.

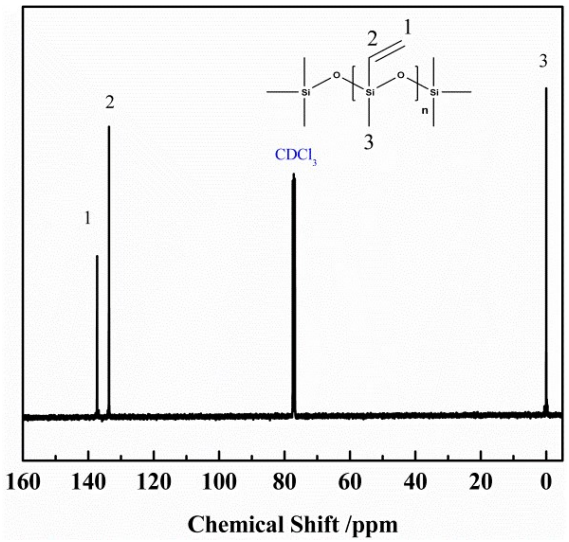

Figure S8 ^{13}C NMR spectrum of PVMS-3.

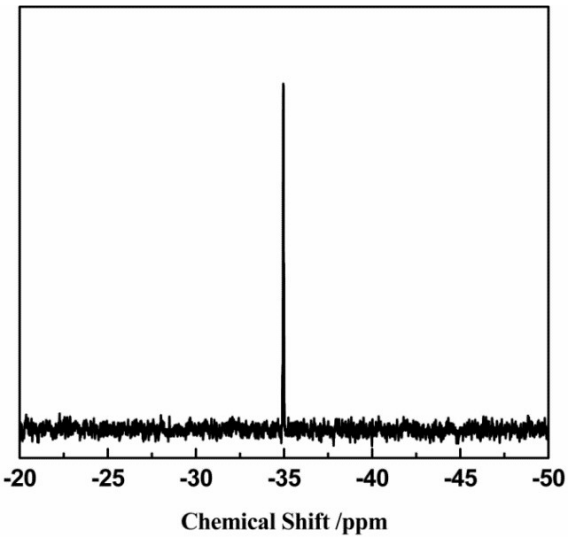

Figure S9 ^{29}Si NMR spectrum of PVMS-3.

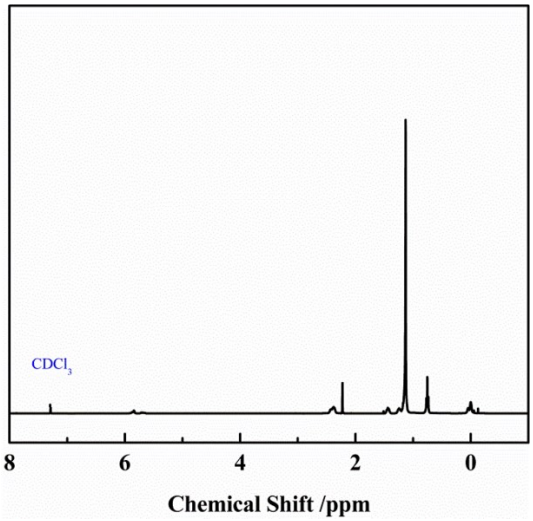

Figure S10 ^{1}H NMR spectrum of $Si_{0.75}$-18-1.

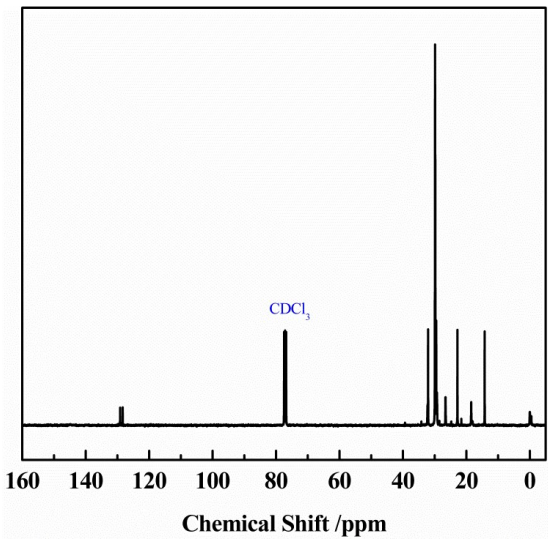

Figure S11 ^{13}C NMR spectrum of $Si_{0.75}$-18-1.

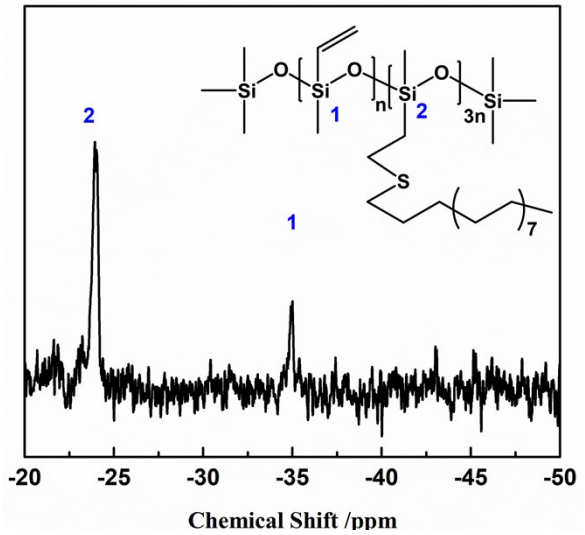

Figure S12 ^{29}Si NMR spectrum of $Si_{0.75}$-18-1.

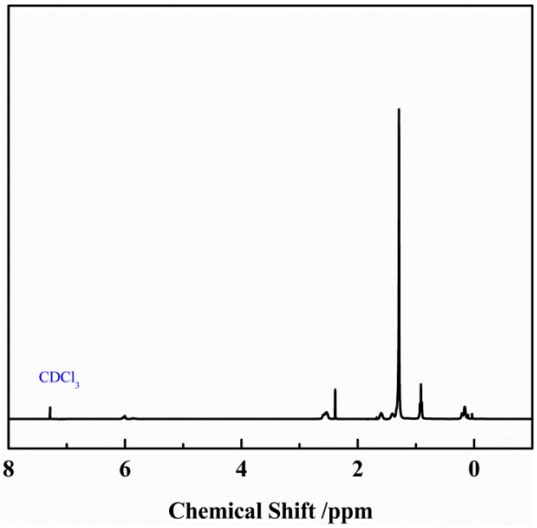

Figure S13 ^{1}H NMR spectrum of $Si_{0.75}$-18-2.

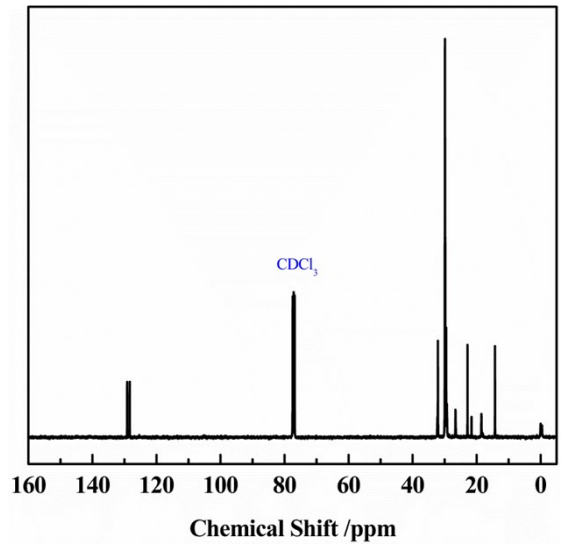

Figure S14 ^{13}C NMR spectrum of $Si_{0.75}$-18-2.

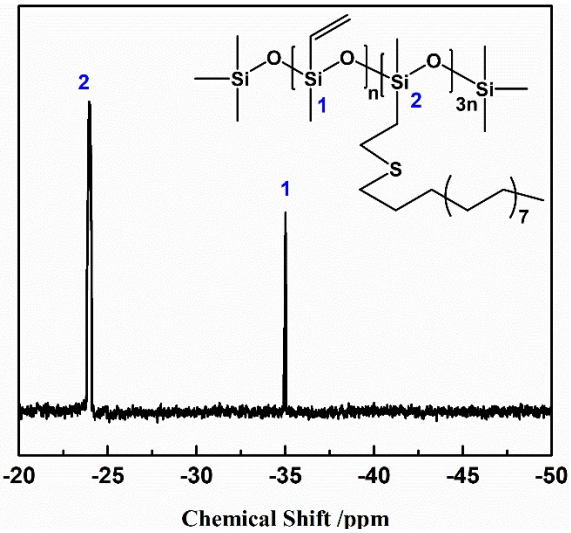

Figure S15 ^{29}Si NMR spectrum of $Si_{0.75}$-18-2.

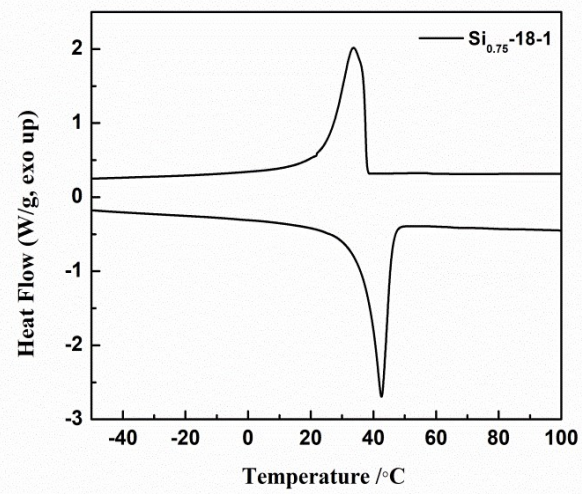

Figure S16 DSC thermogram for $Si_{0.75}$ 18-1.

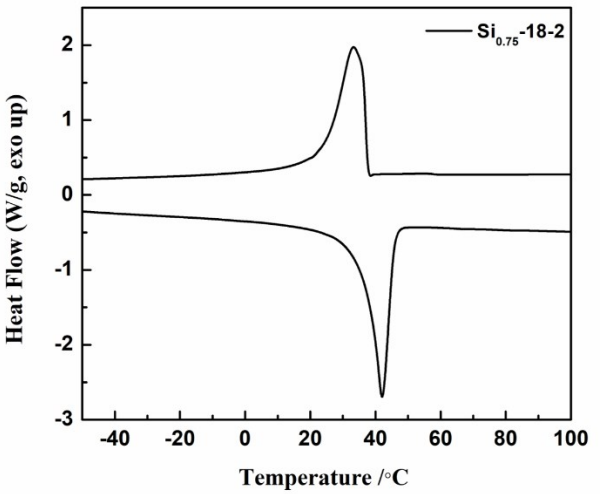

Figure S17 DSC thermogram for $Si_{0.75}$ 18-2.

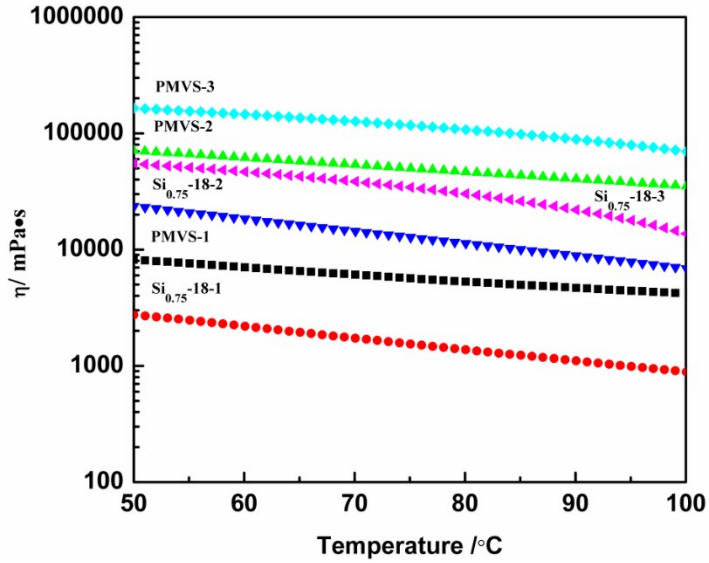

Figure S18 Viscosity-temperature curves of PMVS-x and $Si_{0.75}$-18-x.

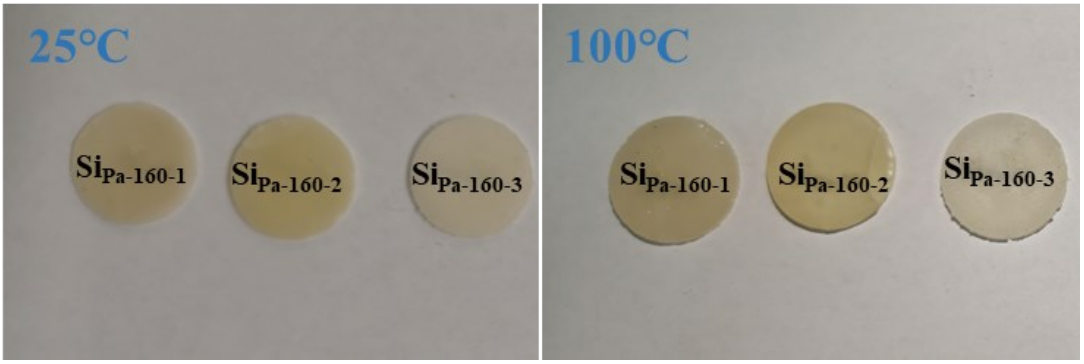

Figure S19 Visual images of $Si_{Pa\text{-}160\text{-}1}$ $Si_{Pa\text{-}160\text{-}2}$ and $Si_{Pa\text{-}160\text{-}3}$ s at 25 °C and 100 °C for 60 min.

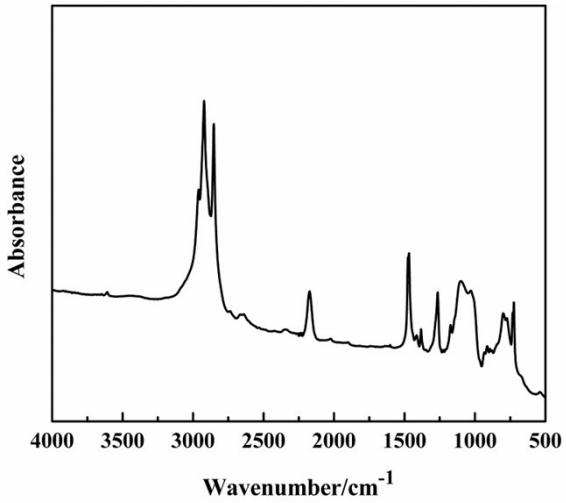

Figure S20 Fourier transform infrared (FT-IR) spectra of $Si_{Pa\text{-}160\text{-}1}$.

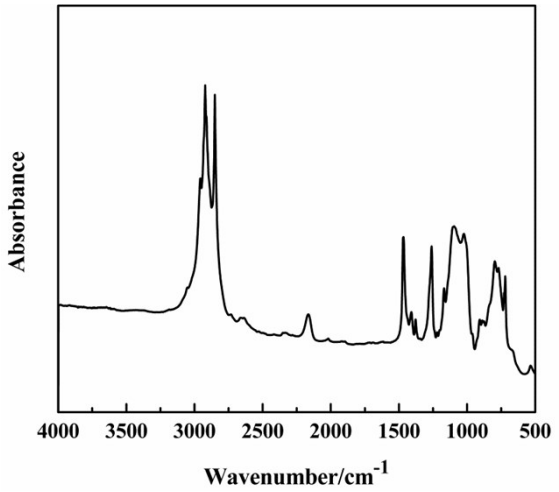

Figure S21 Fourier transform infrared (FT-IR) spectra of $Si_{Pa\text{-}160\text{-}2}$.

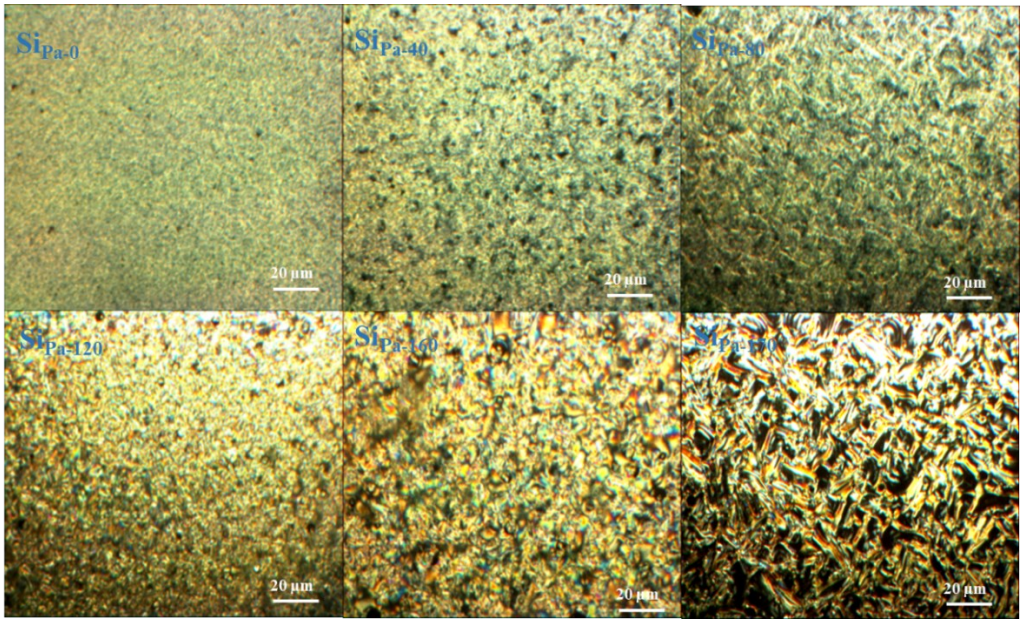

Figure S22 POM images of the $Si_{Pa\text{-}X}$ systems.

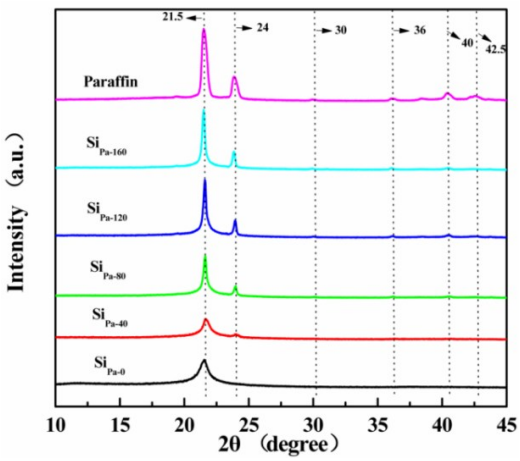

Figure S23 XRD diagrams of the Si_{Pa-X} systems.

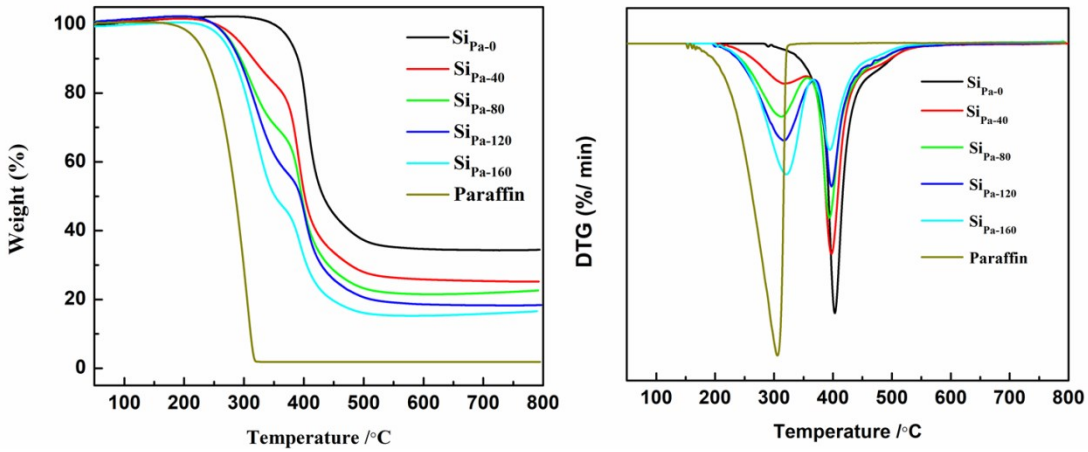

Figure S24 Thermal stability analysis of the Si_{Pa-X} systems.

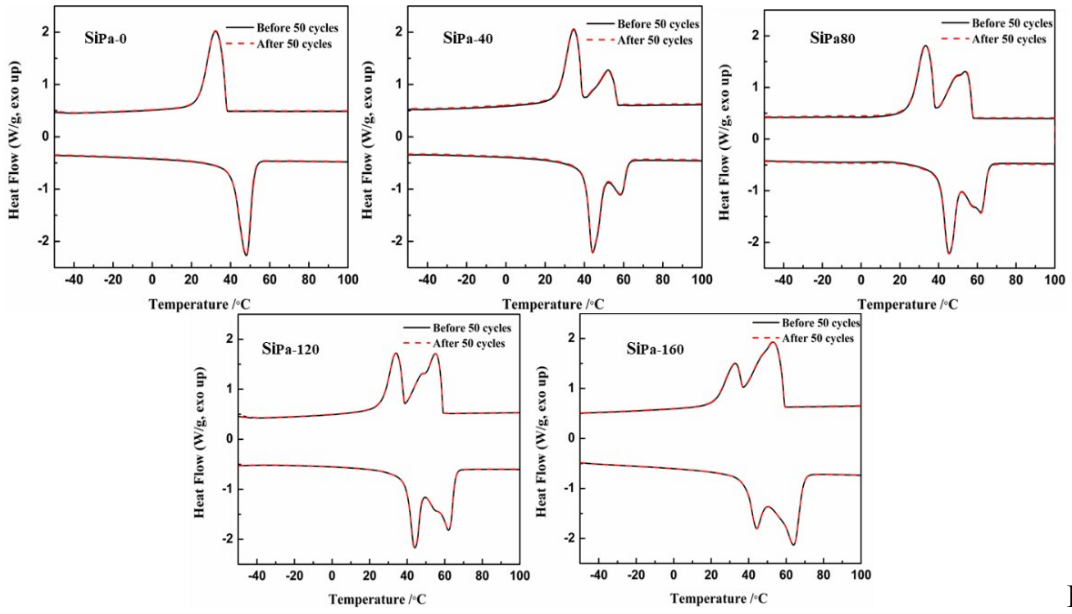

Figure S25 DSC curves of the Si_{Pa-X} systems before and after 50 thermal cycles.

Figure S26 Visual images of uncured $Si_{Pa\text{-}160}$ systems' cyclohexane solution dispersing multi-walled carbon nanotubes.

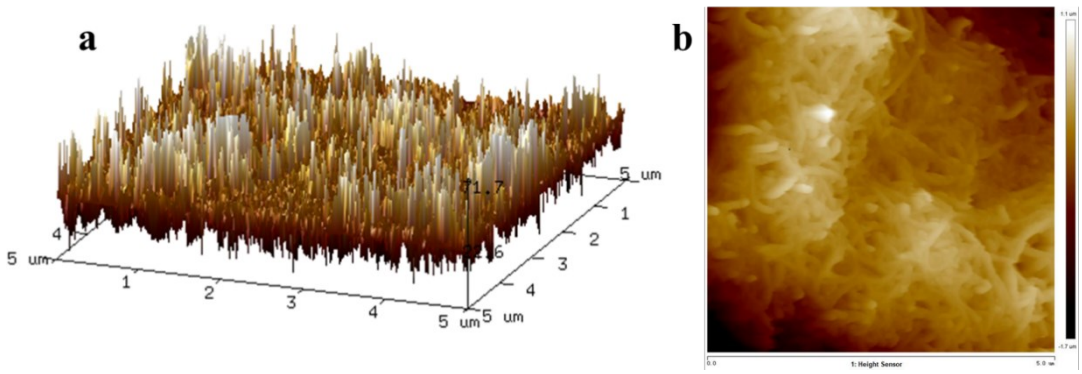

Figure S27 (a) 3D AFM image and (b) Height image of the $Si_{Pa\text{-}160}$/CNTs-3 film surface.

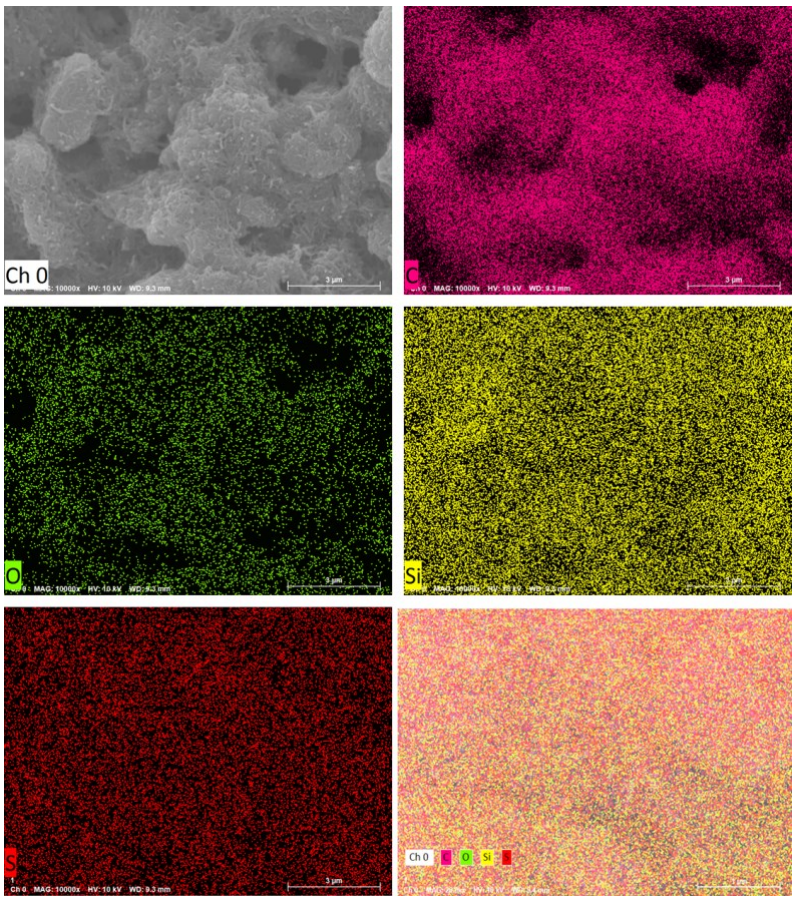

Figure S28 SEM-EDS data of the $Si_{Pa\text{-}160}$/CNTs-3 film surface.

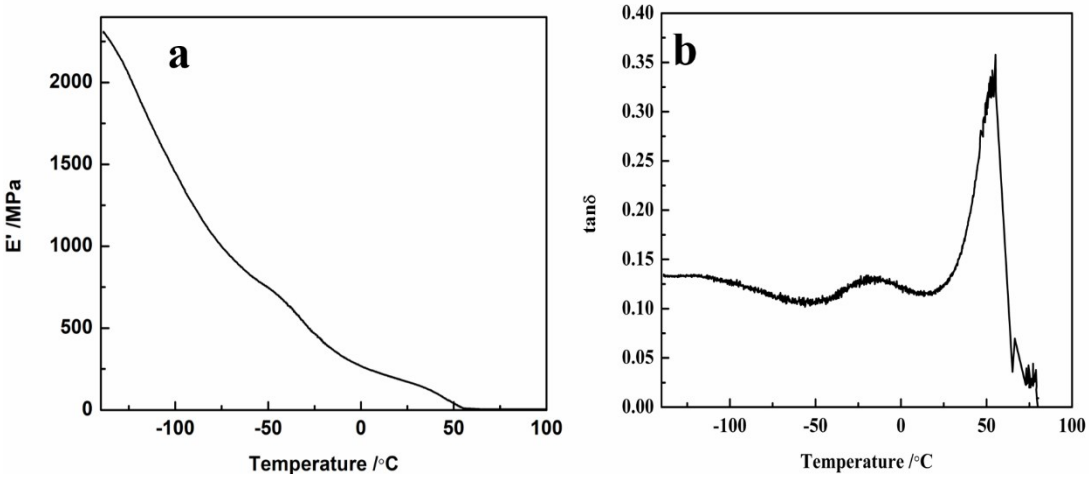

Figure S29 (a) E' and (b) tan δ as a function of temperature for $Si_{0.75}$-18-3 curing network.

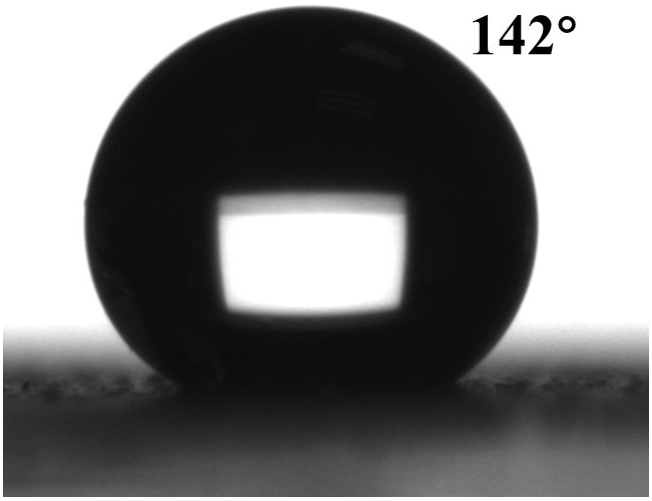

Figure S30 Water contact angles of the $Si_{Pa\text{-}160}$/CNTs-3 film at 70℃.

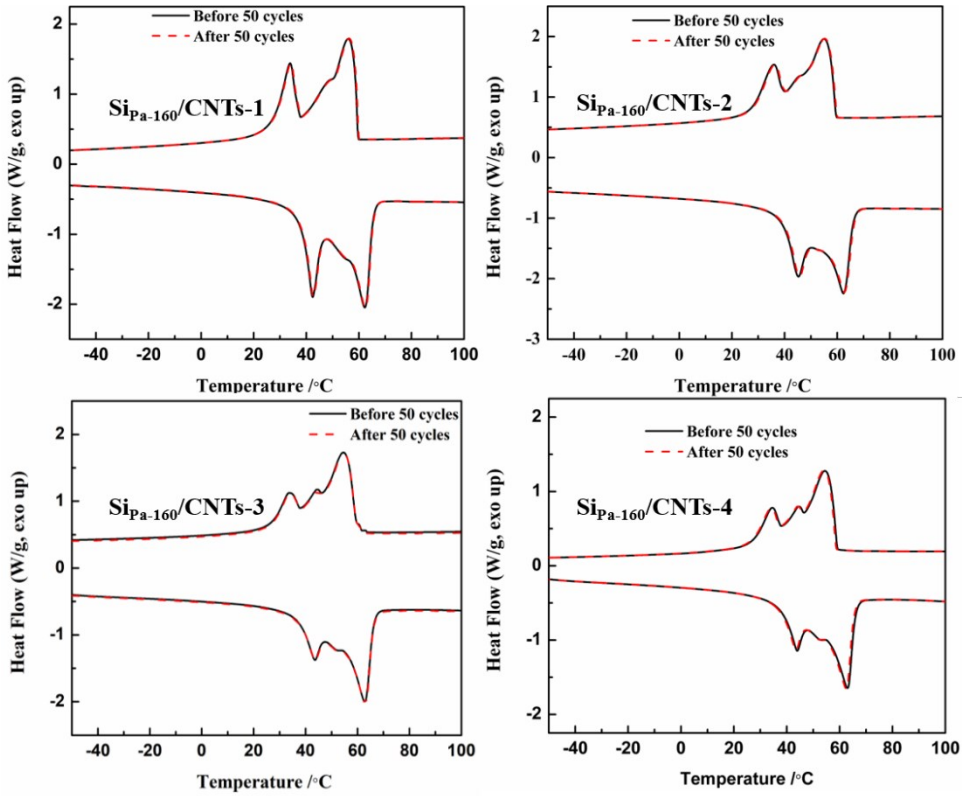

Figure S31 DSC curves of $Si_{Pa\text{-}160}$/CNTs-x before and after 50 thermal cycles.

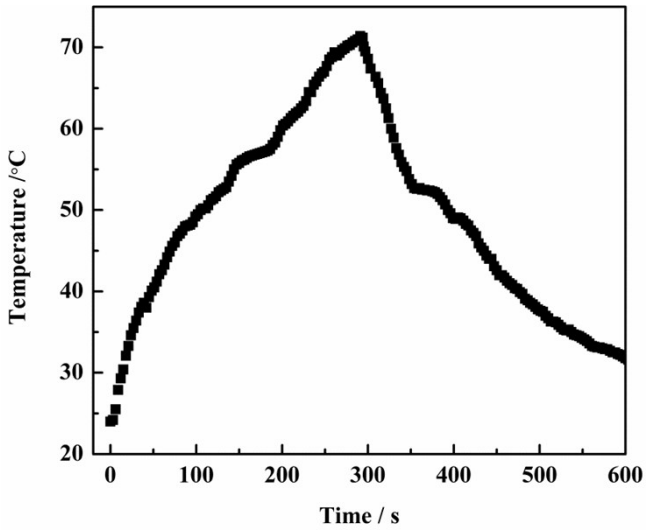

Figure S32 Temperature–time curve of the $Si_{Pa\text{-}160}$/CNTs-3 film after 20 illuminated cycles at 100 mW/cm^{-2}.

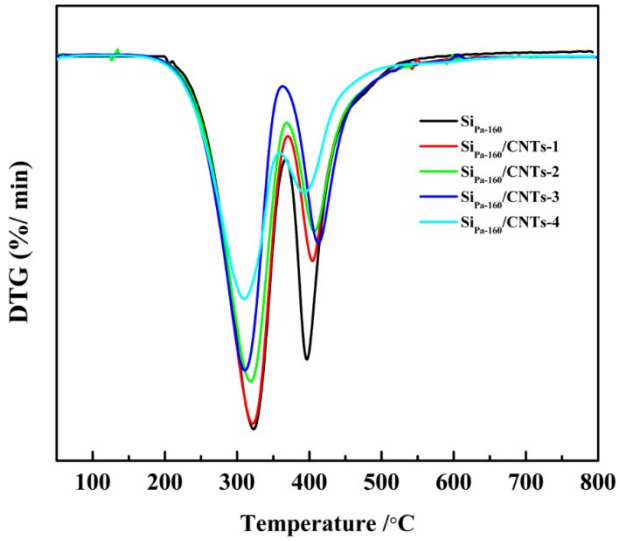

Figure S33 DTG curves of $Si_{Pa\text{-}160}$/CNTs-x.

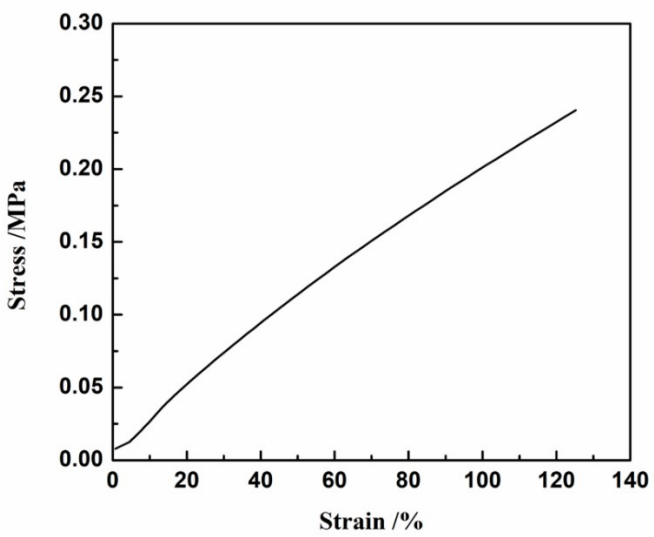

Figure S34 Stress-Strain curve of $Si_{0.75}$-18-3 curing network at 70℃ (measured by DMA).

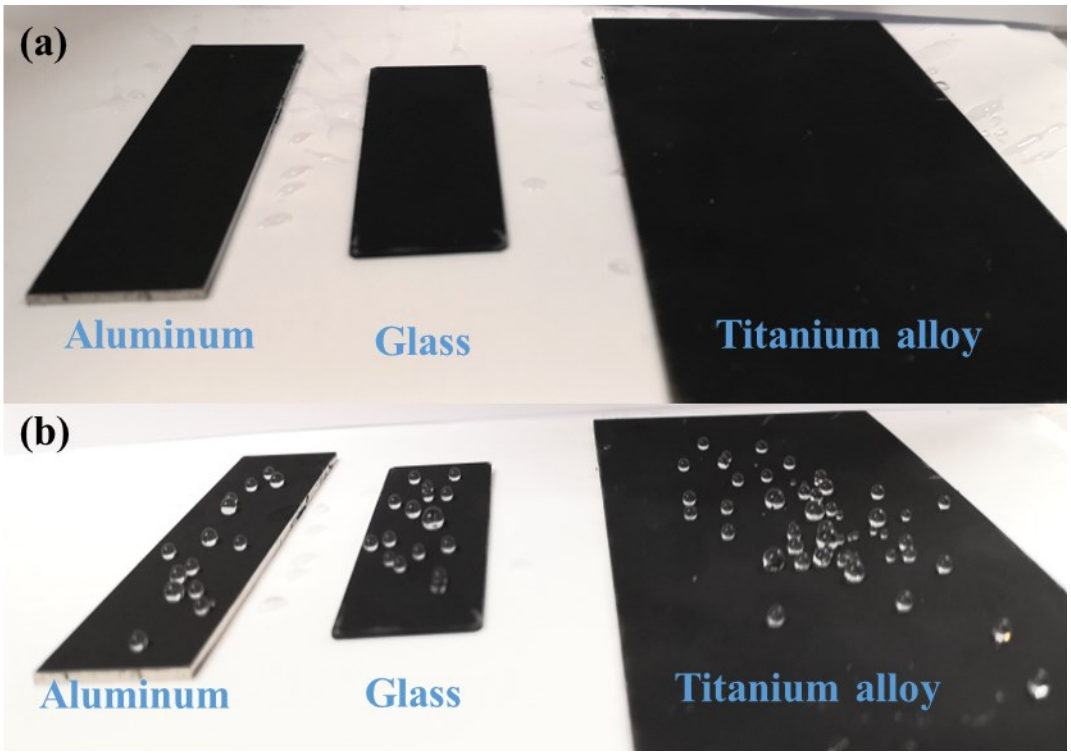

Figure S35 Optical image of the aluminum, glass and titanium alloy substrates coated with $Si_{Pa\text{-}160}$/CNTs-3.

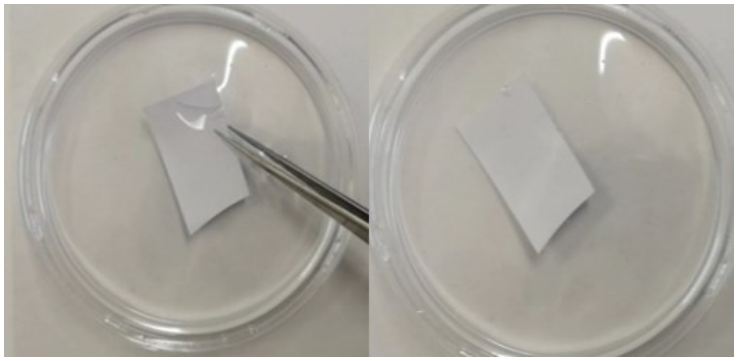

Figure S36 Optical photographs of drag reduction test of the uncoated paper.

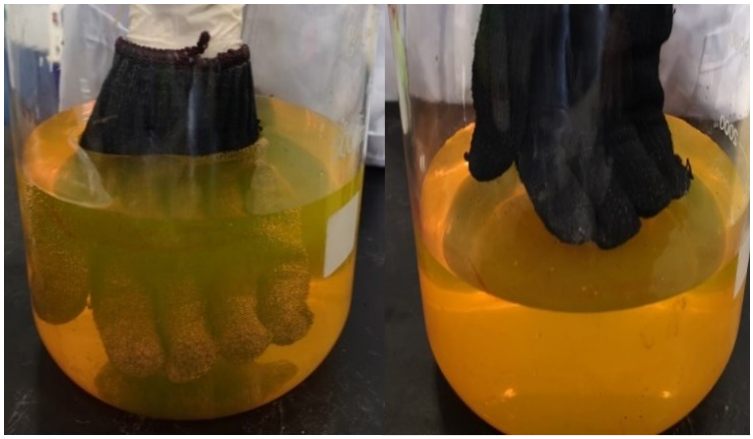

Figure S37 Waterproofing test of the fabric glove treated with $Si_{Pa\text{-}160}$/CNTs-3.

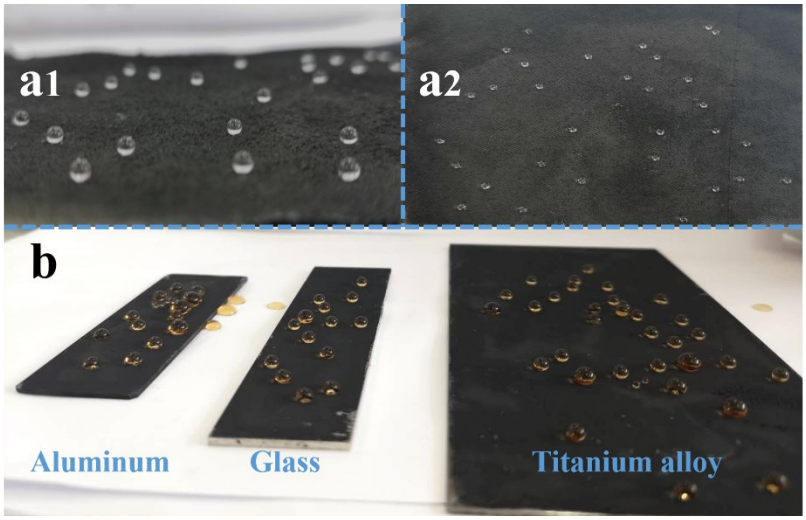

Figure S38 (a) Optical image of the superhydrophobic behavior of the coat treated with $Si_{Pa\text{-}160}$/CNTs-3 after 13 months. (b) Optical image of the superhydrophobic behavior of aluminum, glass and titanium alloy substrates coated with $Si_{Pa\text{-}160}$/CNTs-3 after 16 months (red water).

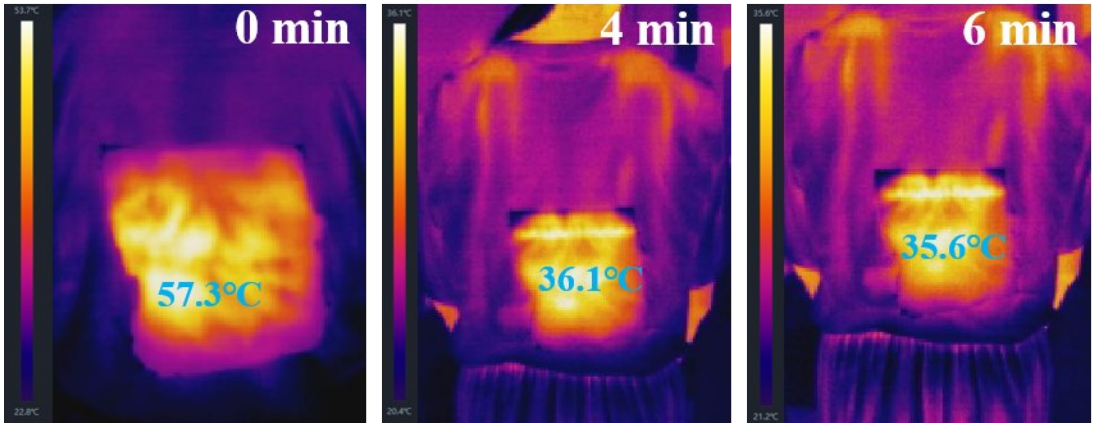

Figure S39 Infrared photo of the treated coat with $Si_{Pa\text{-}160}$/CNTs-3 (cover the back of body) during solar energy conversion and storage.

Supplementary Tables

Table S1 Relative molecular characteristics of PMVS-x and $Si_{0.75}$-18-x.

Sample	Mn[a)]	PDI[a)]	Vinyl content[b)]	ΔE_η (KJ/mol)[c)]
PMVS-1	10000	1.7	99%	13.67
PMVS-2	53200	1.7	98%	15.36
PMVS-3	393000	1.8	99%	14.33
$Si_{0.75}$-18-1	13500	2.2	22%	24.43
$Si_{0.75}$-18-2	61800	2.4	21%	22.85
$Si_{0.75}$-18-3	510000	2.3	22%	25.16

a) Number-average molecular weight and PDI are characterized by GPC; b) Vinyl group content obtained by iodometric titration; c) ΔE_η calculated by rheological data following by Arrhennius equation.

Table S2 Thermal characteristics of all the samples. [a)]

System	Melting Process					Freezing Process				
	T_m-Si (°C)	T_m-Pa (°C)	ΔH_m (Jg^{-1})	ΔHT_m (Jg^{-1})	ΔH_m loss (%)	T_f-Si (°C)	T_f-Pa (°C)	ΔH_f (Jg^{-1})	ΔHT_f (Jg^{-1})	ΔH_m loss (%)
Paraffin	/	60.0	240.0	/	/	/	52.8	222.7	/	/
ODT	31.7	/	240.2	/	/	22.3	/	233.8	/	/
$Si_{0.75}$-18-3	42.2	/	114.4	171.6	33.3	33.3	/	112.9	167.0	32.4
Si_{Pa-0}	44.4	/	97.1	/	/	32.4	/	96.9	/	/
Si_{Pa-40}	44.2	58.1	128.7	136.5	5.7	36.6	52.3	125.7	134.0	6.7
Si_{Pa-80}	44.8	61.6	148.6	158.9	6.5	33.7	54.2	146.5	156.1	6.2
Si_{Pa-120}	44.2	62.6	167.7	173.3	3.2	33.4	54.9	165.2	169.9	2.8
Si_{Pa-160}	44.2	63.8	182.2	183.4	0.7	33.7	53.7	178.3	179.6	0.7
Si_{Pa-160}/CNTs-1	42.3	62.2	164.2	165.6	0.9	33.6	56.0	160.0	162.1	1.3
Si_{Pa-160}/CNTs-2	45.5	62.3	150.3	151.8	1.1	35.9	54.9	146.5	148.6	1.4
Si_{Pa-160}/CNTs-3	43.6	62.8	138.0	140.2	1.5	34.8	54.3	134.3	137.2	2.1
Si_{Pa-160}/CNTs-4	43.8	62.9	126.3	130.1	3.0	37.5	54.2	124.5	127.4	2.3

a) Notes: Tm, Tf, ΔH_m, and ΔH_f can be obtained directly from DSC curves; ΔHT_m and ΔHT_f of $Si_{0.75}$-18-3 were calculated by multiplying the weight percentage of ODT in $Si_{0.75}$-18-3 by the melting or freezing enthalpies of ODT; ΔHT_m and ΔHT_f of the Si_{Pa-x} samples were calculated by summing the melting or freezing enthalpies of the Si_{Pa-0} parts (multiplying the weight percentage of Si_{Pa-0} with the melting or freezing enthalpies of the Si_{Pa-0} sample) and the paraffin parts (multiplying the weight percentage of paraffin with the melting or freezing enthalpies of paraffin); ΔHT_m and ΔHT_f of Si_{Pa-160}/CNTs-x were calculated by multiplying the weight percentage of Si_{Pa-160} in Si_{Pa-160}/CNTs-x by the melting or freezing enthalpies of Si_{Pa-160}.

Table S3 EDS results of Si_{Pa-160}.

Element	Weight (%)	
	Area 1 of Si_{Pa-160} SSPCMs	Area 2 of Si_{Pa-160} SSPCMs
C	96.4	72.5
Si	0.2	15.2
O	1.9	9.9
S	1.5	2.4